

# PROCEEDINGS OF SPIE

[SPIDigitalLibrary.org/conference-proceedings-of-spie](https://SPIDigitalLibrary.org/conference-proceedings-of-spie)

## Camera feedback optimization of computer-generated holograms displayed by the Texas Instruments phase light modulator for AR/HUD applications

Remington Ketchum, Tianyao Zhang, Pierre-Alexandre Blanche

Remington S. Ketchum, Tianyao Zhang, Pierre-Alexandre Blanche, "Camera feedback optimization of computer-generated holograms displayed by the Texas Instruments phase light modulator for AR/HUD applications," Proc. SPIE 12231, ODS 2022: Industrial Optical Devices and Systems, 1223109 (30 September 2022); doi: 10.1117/12.2633114

**SPIE.**

Event: SPIE Optical Engineering + Applications, 2022, San Diego, California, United States

# Camera feedback optimization of computer generated holograms displayed by the Texas Instruments Phase light modulator for AR/HUD applications.

Remington S. Ketchum<sup>a</sup>, Tianyao Zhang<sup>a</sup>, and Pierre-Alexandre Blanche<sup>a</sup>

<sup>a</sup>University of Arizona, James C. Wyant College of Optical Sciences, 1630 E University Blvd., Tucson, AZ 85721, USA

## ABSTRACT

Computer generated holograms (CGHs) used for AR/VR displays typically have poor image quality compared to their numerical reconstructions. The primary cause of these discrepancies can be attributed to over idealized wave propagation used for CGH generation. This problem is often exacerbated when the image is projected through a more complex optical system like a holographic waveguide combiner or using the Texas Instruments phase light modulator (PLM) that has nonlinear phase levels. Direct camera feedback during hologram optimization has been shown to significantly improve image quality for CGHs projected in free space. Here we demonstrate the use of camera feedback optimization for improving image quality of CGHs projected through holographic waveguide combiners and using the TI PLM as phase SLM. Machine learning can be applied to create adjust the numerical propagation method to closer match physical propagation through the system without the need for camera feedback after training. This method corrects for various optical aberrations, beam profile, and phase nonlinearities in the display. Further image improvement is made by leveraging high speed MEMS based PLM for time multiplexing CGHs to reduce speckle. Application of these techniques for different waveguide geometries (i.e. planar and curved) will be discussed.

**Keywords:** Holography, CGH, HOE, Waveguide Combiner

## 1. INTRODUCTION

Waveguide combiners are useful tools in AR/VR applications because they allow for an expanded eyebox without sacrificing the field of view. This is possible due to pupil expansion in which a single entrance pupil is replicated by partially extracting light upon each internal reflection across an outcoupler. Pupil expansion can be extended to 2D by including a redirection, or fold, grating to partially redirect light while continuing to propagate through the waveguide. The concept of a holographic waveguide combiner and a physical demonstrator are shown in Fig. 1.<sup>1,2</sup> Propagation through a waveguide combiner can have negative impacts on image quality. The holographic couplers can add haze or aberrations into the image. Imperfect surface quality of the waveguide can also introduce scattering and light leakage during propagation.

The Texas Instruments phase-only spatial light modulator (TI-PLM) is a MEMS based phase modulator that uses vertically actuated MEMS mirrors to modulate the phase of a reflected wavefront.<sup>3,4</sup> Device properties for the TI-PLM are presented in Tab. 1. While theoretically 16 phase levels can produce a high (~98%) diffraction efficiency for simple gratings, due to the nonlinear distribution of the phase levels and overall mirror morphology, the TI-PM can only achieve 85% diffraction efficiency (with respect to the undiffracted zeroth order) for a simple blazed grating.<sup>5</sup> The same limitations in phase levels and the mirror morphology also has a strong impact on the image quality of images produced from a CGH projected by the TI-PLM.

Due to the high speed and reliability offered by the MEMS technology, the TI-PLM is a promising candidate for holographic display engines. The high speed can be used to help artificially expand the space-bandwidth

---

Further author information: (Send correspondence to R.S.K)  
R.S.K.: E-mail: rsketchum@optics.arizona.edu

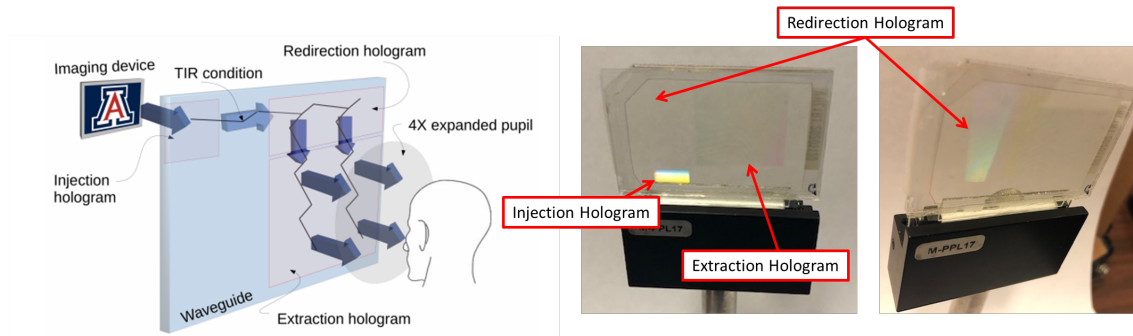


Figure 1. Principle of 2D pupil expansion using holographic waveguide combiner, (left) and physical waveguide used for testing (right).

product of the display to ultimately improve the quality of 3D images that can be produced by CGHs.

Table 1. TI-PLM device properties.

0.67" TI-PLM	
Resolution	1280 x 800
Mirror size	10.5 $\mu\text{m}$ x 10.5 $\mu\text{m}$
Mirror pitch	10.8 $\mu\text{m}$ x 10.8 $\mu\text{m}$
Number of phase levels	16

Here we evaluate the performance of the TI-PLM for projecting CGH based 2D images through a holographic 2D planar waveguide and test the ability of camera-in-the-loop (CITL) algorithms to improve image quality in this system. The algorithms are adapted from Peng et al.<sup>6</sup> and modified for the TI-PLM. The method uses a stochastic gradient descent (SGD) optimizer as part of an iterative Fourier transform algorithm (IFTA) to optimize a CGH pattern using the angular spectrum method (ASM) of propagation. Camera-in-the-loop (CITL) optimization uses direct camera feedback of optically reconstructed holograms on each iteration to account for the non-ideal propagation through the physical optical system.

## 2. METHODS

### 2.1 Optical setup

The testing setup is illustrated in Fig. 2 and consists of an expanded and collimated CW laser source (532 nm). A rotating diffuser at the confocal point of the collimation optics is used to reduce laser speckle. The collimated beam illuminates the PLM at normal incidence through a non-polarizing cube beam splitter. The reflected wavefront is directed back through the beam splitter and redirected towards the waveguide system. A set of lenses set up as a telescope is used to demagnify the image and set it to infinity to couple into the waveguide at the injection hologram. After propagating through the waveguide, the image is extracted through an extraction hologram and imaged using a CCD camera (AmScope MU1803) with a double Gauss lens focused to infinity.

The waveguide combiner (Fig. 1) consists of three HOEs recorded by two beam interference into a photopolymer as described in the literature.<sup>1</sup> The first HOE is an injection hologram used to couple the image into the waveguide, the second HOE is a redirection hologram that rotates the propagating light by 90° within the

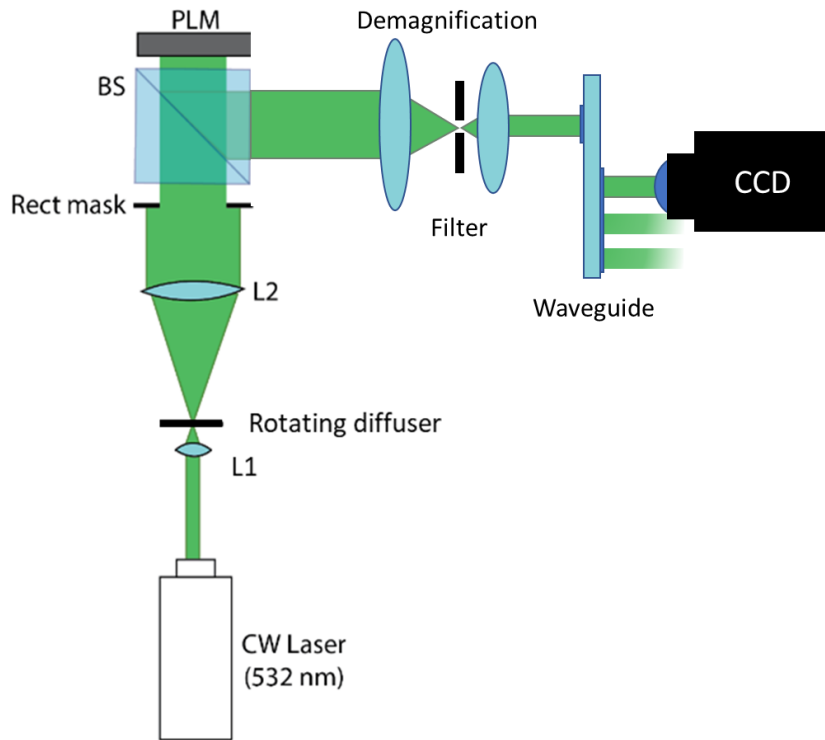


Figure 2. Optical setup for displaying holograms.

waveguide, and the third HOE is an extraction hologram used to outcouple the light (with 2D pupil expansion). The PLM and the camera are controlled by a computer running the CITL optimization routines.

## 2.2 Image quality analysis

Image quality is assessed using three metrics: peak signal-to-noise ratio (PSNR), structural similarity index measure (SSIM), and speckle contrast (SC). PSNR is defined as,

$$PSNR = 10 \log \left( \frac{255^2}{MSE} \right) \quad (1)$$

Where, MSE is the mean squared error between the target image and the optically reconstructed image. PSNR is on a decibel scale and higher PSNR values correspond with closer reconstruction of the target image. PSNR is a direct pixel by pixel comparison that does not take human vision subjectivity into account. SSIM is a perception-based metric that incorporates luminance, contrast, and structural difference between two images.<sup>7</sup>

$$SSIM(x, y) = l(x, y)^\alpha \cdot c(x, y)^\beta \cdot s(c, y)^\gamma \quad (2)$$

where,

$$l(x, y) = \frac{2\mu_x\mu_y + C_1}{\mu_x^2 + \mu_y^2 + C_1} \quad (3)$$

$$c(x, y) = \frac{2\sigma_x\sigma_y + C_2}{\sigma_x^2 + \sigma_y^2 + C_2} \quad (4)$$

$$s(x, y) = \frac{\sigma_{xy} + C_3}{\sigma_x \sigma_y + C_3} \quad (5)$$

SSIM values range from 0 to 1 where a value of 1 corresponds to exact reproduction of the target image. The three components of SSIM can be weighted differently using  $\alpha$ ,  $\beta$ , and  $\gamma$  to prioritize certain components. For this study,  $\alpha = \beta = \gamma = 1$ . While the SSIM is localized over the entire image, the result is typically presented as the mean of the SSIM (MSSIM) values. Calculation of the SSIM is done using a moving window approach to account for slight misalignment and distortions.

Since the projection system used involves coherent light, the resulting images are subject to laser speckle. Laser speckle is commonly quantified by the ratio of the standard deviation of intensity to the mean intensity over a region:<sup>8</sup>

$$SC = \frac{\sigma}{\mu} \quad (6)$$

SC values range from 0 to 1 where a 0 corresponds to no speckle noise and a 1 corresponds to an image entirely of speckle noise.

### 3. RESULTS AND DISCUSSION

A set of 100 images from the DIV2K dataset<sup>9</sup> were used to generate CGHs with and without CITL. A sample of these images is shown in Fig. 3.

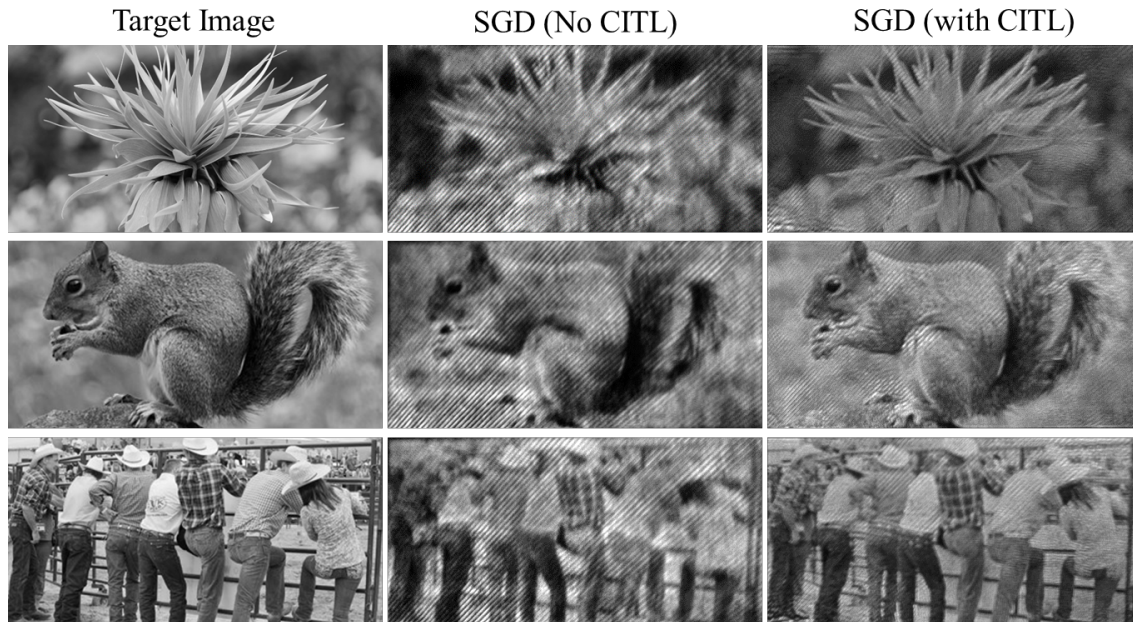


Figure 3. Target images and optical reconstructions of the corresponding CGHs imaged through a planar waveguide with and without CITL optimization.

Qualitatively Fig. 3 illustrates the ability of CITL to drastically improve image quality after propagation through a planar waveguide combiner. Aberrations, uniformity of illumination, and unwanted interference fringes from the waveguides are all noticeably improved. Quantitatively, the SSIM, PSNR, and SC demonstrate significant improvement in image quality for the test set of 100 images as shown in Fig. 4.

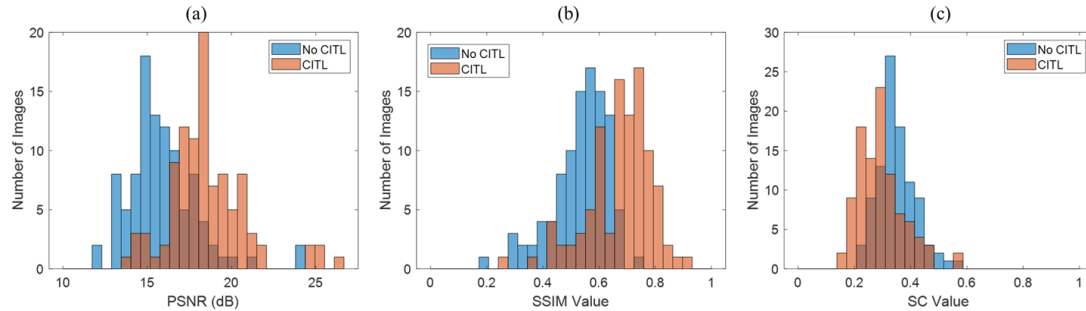


Figure 4. a) PSNR, b) SSIM, and c) SC distributions for 100 test images.

Using CITL, on average, the SSIM increased 25.6% from 0.54 to 0.67, the PSNR increased 2.65 decibels from 15.9 dB to 18.5 dB, and the SC decreased by 15.3% from 0.35 to 0.30. This indicates significant improvement for all three metrics.

#### 4. CONCLUSION

Here we have evaluated the TI-PLM for use as a display in a laser light engine for a holographic waveguide combiner. Image quality degradation due to input/output coupling and propagation through the waveguide were corrected using CITL optimization for 2D CGH generation. This was demonstrated qualitatively and was reflected in improvements in the PSNR, SSIM, and SC of images produced by the CGHs. Leveraging the high speed of the TI-PLM, SC and PSNR could be further improved by time multiplexing CGH patterns generated using different random phase seeds.

Future work will look at the uniformity of image quality across multiple exit pupils. This includes the impact of CITL optimization for one exit pupil's impact on other exit pupils. Other waveguide geometries, including curved waveguide combiners, will also be considered.

#### REFERENCES

- [1] Draper, C. T., Bigler, C. M., Mann, M. S., Sarma, K., and Blanche, P.-A., "Holographic waveguide head-up display with 2-D pupil expansion and longitudinal image magnification," *Applied Optics* **58**(5), A251 (2019).
- [2] Bigler, C. M., Mann, M. S., and Blanche, P.-A., "Holographic waveguide HUD with in-line pupil expansion and 2D FOV expansion," *Applied Optics* **58**(34), G326 (2019).
- [3] Bartlett, T. A., McDonald, B. C., and Hall, J., "Adapting Texas Instruments DLP technology to demonstrate a phase spatial light modulator," 27 (2019).
- [4] Bartlett, T. A., McDonald, W. C., Hall, J. N., Oden, P. L., Doane, D., Ketchum, R. S., and Byrum, T., "Recent advances in the development of the Texas Instruments phase-only microelectromechanical systems (MEMS) spatial light modulator," 20 (2021).
- [5] Ketchum, R. S. and Blanche, P. A., "Diffraction efficiency characteristics for MEMS-based phase-only spatial light modulator with nonlinear phase distribution," *Photonics* **8**(3), 1–9 (2021).
- [6] Peng, Y., Choi, S., Padmanaban, N., and Wetzstein, G., "Neural holography with camera-in-the-loop training," *ACM Transactions on Graphics* **39**(6) (2020).
- [7] Wang, Z., Bovik, A. C., Sheikh, H. R., and Simoncelli, E. P., "Image quality assessment: From error visibility to structural similarity," *IEEE Transactions on Image Processing* **13**(4), 600–612 (2004).
- [8] Liang, C., Zhang, W., Wu, Z., Rui, D., Sui, Y., and Yang, H., "Beam shaping and speckle reduction in laser projection display systems using a vibrating diffractive optical element," *Current Optics and Photonics* **1**(1), 23–28 (2017).
- [9] Agustsson, E. and Timofte, R., "NTIRE 2017 Challenge on Single Image Super-Resolution: Dataset and Study," in [*IEEE Computer Society Conference on Computer Vision and Pattern Recognition Workshops*], **2017-July**, 1122–1131 (2017).